dium," *International Journal of Heat and Mass Transfer*, Vol. 28, No. 8, 1985, pp. 1597–1611.

[5]Lai, F. C., "Coupled Heat and Mass Transfer by Natural Convection from a Horizontal Line Source in Saturated Porous Medium," *International Communications in Heat and Mass Transfer*, Vol. 17, No. 4, 1990, pp. 489–499.

[6]Lai, F. C., and F. A. Kulacki, "Coupled Heat and Mass Transfer by Natural Convection from Vertical Surfaces in Porous Media," *International Journal of Heat and Mass Transfer*, Vol. 34, No. 4/5, 1991, pp. 1189–1194.

[7]Jang, J.-Y., and Chang, W.-J., "The Flow and Vortex Instability of Horizontal Natural Convection in a Porous Medium Resulting from Combined Heat and Mass Buoyancy Effects," *International Journal of Heat and Mass Transfer*, Vol. 31, No. 4, 1988, pp. 769–777.

[8]Jang, J.-Y., and Chang, W.-J., "Buoyancy-Induced Inclined Boundary Layer Flow in a Porous Medium Resulting from Combined Heat and Mass Buoyancy Effects," *International Communications in Heat and Mass Transfer*, Vol. 15, No. 1, 1988, pp. 17–30.

[9]Yucel, A., "Natural Convection Heat and Mass Transfer Along a Vertical Cylinder in a Porous Medium," *International Journal of Heat and Mass Transfer*, Vol. 33, No. 10, 1990, pp. 2265–2274.

[10]Lai, F. C., Choi, C. Y., and Kulacki, F. A., "Coupled Heat and Mass Transfer by Natural Convection from Slender Bodies of Revolution in Porous Media," *International Communications in Heat and Mass Transfer*, Vol. 17, No. 5, 1990, pp. 609–620.

[11]Gebhart, B., Jaluria, Y., Mahajan, R. L., and Sammakia, B., *Buoyancy-Induced Flows and Transport*, Hemisphere, New York, 1988, pp. 54–64.

[12]Cheng, P., and Chang, I.-D., "Buoyancy Induced Flows in a Saturated Porous Medium Adjacent to Impermeable Horizontal Surfaces," *International Journal of Heat and Mass Transfer*, Vol. 19, No. 11, 1976, pp. 1267–1272.

Heat (Mass) Transfer in a Rotating Channel with Ribs of Various Sizes on Two Walls

C. W. Park,* S. C. Lau,† and R. T. Kukreja‡
Texas A&M University, College Station, Texas 77843

Introduction

NAPHTHALENE sublimation experiments have been conducted to study the effect of rib size on the heat (mass) transfer for radial outward flow in a rotating square channel with transverse ribs on the leading and trailing walls. The test channel modeled internal turbine blade cooling passages. Results were obtained for a Reynolds number Re of 5.5×10^3 and a rotation number Ro of 0.24, both of which were based on the hydraulic diameter of the test channel D.

Because the variation of the density of the naphthalene vapor–air mixture that passed through the test channel during an experiment was negligible, only the effects of the Coriolis force and the rib size, but not the buoyancy force, were examined. The results of this investigation may be used to improve numerical models for the design of cooling channels in turbine blades. The results should also help researchers and engineers better understand the effect of rib size on the heat (mass) transfer on the leading and trailing walls of a rotating channel.

Received Sept. 8, 1997; revision received Jan. 2, 1998; accepted for publication Jan. 13, 1998.

*Postdoctoral Associate, Mechanical Engineering.
†Associate Professor, Mechanical Engineering.
‡Research Engineer, Lynntech Inc., 7610 Eastmark Drive.

Test Apparatus and Procedure

The test apparatus, the instrumentation, and the test procedure for this study are the same as those used in Park et al.[1] Only a brief description is given in this Note.

The test section was an aluminum two-pass channel with a square cross section of 1.59 by 1.59 cm. The two straight segments were 0.11 m long. Naphthalene in shallow cavities covered the inner surfaces of the individual walls of the test section, so that the exposed surfaces of the test section walls were all mass transfer active during an experiment. In this investigation, attention was focused on the first straight pass only.

Ribs were cut from square balsa wood strips. The ribs were attached with epoxy transversely on two opposite walls of the first straight pass of the test channel. The exposed surfaces of the ribs were coated with naphthalene. The height of the ribs e ranged from 1/32 to 1/10 of the test channel hydraulic diameter. The rib arrays on the two walls were aligned. The rib spacing, or the pitch p, was equal to the test channel hydraulic diameter.

An entrance channel and an exit channel had the same square cross section as the test section and had lengths of 10 and 20 hydraulic diameters, respectively. The test section along with the entrance and exit channels rotated in a horizontal plane, with respect to a vertical axis, in a steel protective cage. The mean rotating radius of the test section was 30 times the test channel hydraulic diameter.

During a test run local elevation changes were measured at a grid of points on the naphthalene-coated surface of each of the two rib-roughened walls (537 points on each wall; 54 points between two ribs: 9 points along 6 lines that were parallel to the rib axes).

The local mass transfer coefficient is evaluated at each measurement point from the change of elevation at the point, the duration of the test run, and the difference between the naphthalene vapor density at the wall and the local bulk density of naphthalene in the airstream. The Sherwood number Sh is a dimensionless mass transfer coefficient based on the test channel hydraulic diameter and the diffusion coefficient for naphthalene vapor in air.[2] The Sherwood number is normalized by the corresponding Sherwood number for fully developed turbulent flow through a stationary smooth tube, $Sh_0 = 0.023Re^{0.8}Sc^{0.4}$. By applying the analogy between heat and mass transfer

$$Nu/Nu_0 = Sh/Sh_0 \tag{1}$$

where Nu is the Nusselt number and $Nu_0 = 0.023Re^{0.8}Pr^{0.4}$. Therefore, the normalized Sherwood number in this study may be considered as the ratio of the heat transfer coefficient for turbulent flow in a rotating square channel to that for the corresponding fully developed turbulent flow in a stationary tube with a hydraulic diameter equal to that of the square channel.

The maximum uncertainty of the Sherwood number is estimated to be 12.2%. The uncertainty of the Reynolds number is found to be 4.8%. The details of the data reduction procedure and the estimation of the experimental uncertainties are available in Park.[3]

In this Note attention is focused on the streamwise variations of the spanwise average Sherwood number ratio ($\overline{Sh}/Sh_0$) and the overall average Sherwood number ratios ($\overline{\overline{Sh}}/Sh_0$) on the leading and trailing walls over a typical pitch between two ribs. The detailed local mass transfer results and other average mass transfer results that are not included here are available in Park.[3]

Presentation and Discussion of Results

To examine the effect of varying the size of the trailing-wall ribs on the mass transfer on the leading and trailing walls, results have been obtained with leading-wall ribs of a fixed size (with either $D/e = p/e = 10$ or 16) and trailing-wall ribs

of various sizes [with $D/e = p/e = 10$, 16, 32, and ∞ (no ribs)]. In Fig. 1, the streamwise variations of $\overline{Sh}/Sh_0$ on the leading and trailing walls are presented over a typical pitch between two ribs that are located at the streamwise coordinates X/D = 5.0 and 6.0. The spanwise-average Sherwood number ratio is the average of the values of Sh/Sh_0 at the nine points along each of the six grid lines between the two ribs. In the figure, open and darkened symbols indicate the mass transfer on the leading and trailing walls, respectively.

Figure 1 clearly shows that the mass transfer for the radial outward flow is higher on the trailing wall than on the leading wall, as rotation shifts the high-velocity, low-concentration core flow toward the trailing wall. Roughening the trailing wall with ribs or increasing the size of the trailing-wall ribs increases the mass transfer on the leading wall. This increase of the leading-wall mass transfer may be the result of the reduction of the rotation-induced asymmetry of the streamwise velocity profile by the periodic local disturbances near the trailing wall with ribs. With the test channel rotating at a relatively high speed (Ro = 0.24 in this study), however, the $\overline{Sh}/Sh_0$ values on the leading wall are much lower than those on the trailing wall, regardless of the size of the trailing-wall ribs.

Figure 2 gives the overall averages of the leading-wall and trailing-wall Sh/Sh_0 values between two ribs at X/D = 5.0 and 6.0. The $\overline{\overline{Sh}}/Sh_0$ results again show that increasing the size of the ribs on the trailing wall increases the mass transfer on the leading wall. For instance, with the smaller ribs ($D/e = p/e$ = 16) on the leading wall, the leading-wall $\overline{\overline{Sh}}/Sh_0$ value increases from 0.48 to 0.97 and 1.25, respectively, when ribs with $D/e = p/e$ = 16 and ribs with $D/e = p/e$ = 10 are added to the trailing wall.

Figure 2 also shows that the overall average mass transfer for the radial outward flow is much lower on the leading wall than on the trailing wall, regardless of the sizes of the ribs on the two walls. The mass transfer on the leading wall, even with ribs, is lower than the mass transfer on the trailing wall without ribs. For a fixed rib configuration ($D/e = p/e$ = 10 or 16) on the leading wall, the smaller ribs with $D/e = p/e$ = 16 on the trailing wall cause slightly higher trailing-wall mass transfer than the larger ribs with $D/e = p/e$ = 10 on the trailing wall. The smaller ribs should require a lower pumping power.

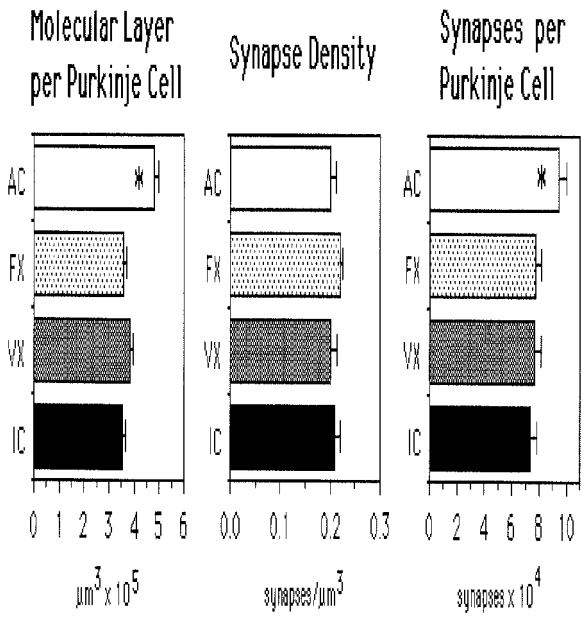

Fig. 1 Streamwise variations of $\overline{Sh}/Sh_0$ between X/D = 5.0 and 6.0 on the leading and trailing walls: leading-wall ribs with a) $D/e = p/e$ = 16 and b) $D/e = p/e$ = 10, and trailing-wall ribs of various sizes.

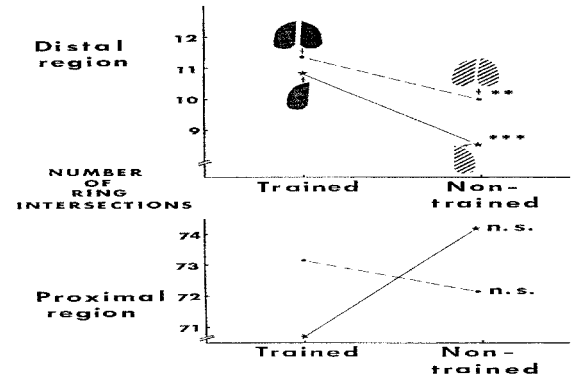

Fig. 2 Variation of $\overline{\overline{Sh}}/Sh_0$ with the size of the ribs on the trailing wall: leading-wall ribs with $D/e = p/e$ = 16 and 10.

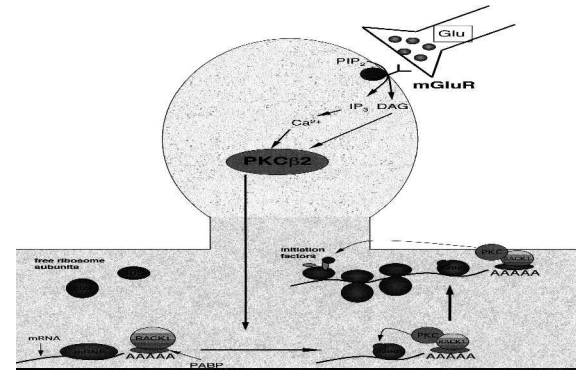

Fig. 3 Streamwise variations of $\overline{Sh}/Sh_0$ between X/D = 5.0 and 6.0 on the leading and trailing walls: trailing-wall ribs with $D/e = p/e$ = 10 and leading-wall ribs of various sizes.

Figure 3 demonstrates the effect of varying the size of the leading-wall ribs on the mass transfer on the leading and trailing walls. The figure presents the streamwise variations of $\overline{Sh}/Sh_0$ between two ribs at X/D = 5.0 and 6.0 with trailing-wall ribs of a fixed size (with $D/e = p/e$ = 10) and leading-wall ribs of various sizes [with D/e or p/e = 10, 16, and ∞ (no ribs)]. With the channel rotating at a relatively high speed and ribs of a fixed size on the trailing wall, the trailing-wall mass transfer is not affected by the surface condition on the leading wall. The relatively small change of the trailing-wall mass transfer shows that roughening the leading wall with ribs or varying the size of the ribs on the leading wall may not significantly change the Coriolis-force-induced asymmetric flowfield. With the channel rotating at a relatively high speed the increased disturbance on the leading wall may not affect the near-wall flow on the rib-roughened trailing wall.

Based on the results of this study, the leading-wall heat (mass) transfer is much lower than the trailing-wall heat (mass) transfer for radial outward flow in a straight channel rotating at a relatively high speed, regardless of the rib configurations on the leading and trailing walls. It is recommended that, in the case of radial outward flow, the surface area or width of the leading wall of a straight pass of a serpentine cooling passage in a gas turbine airfoil be minimized. On the other hand, the surface area or width of the leading wall of an adjacent straight pass with radial inward flow may be increased to take advantage of the high heat transfer on the leading wall when the Coriolis force is reversed. More extensive experimental studies are needed to enable better understanding of the effects of the cross-sectional shape of a rotating channel and the orientations of the walls of the channel on the local heat transfer distributions on the walls.

Concluding Remarks

The effects of rib size on the heat (mass) transfer on the leading and trailing walls of a rotating turbine blade cooling

channel model have been investigated. For radially outward flow with $Re = 5.5 \times 10^3$ and $Ro = 0.24$, and transverse ribs of various sizes up to $D/e = p/e = 10$ on the leading and trailing walls, the following conclusions may be drawn:

1) For a fixed rib configuration on the leading wall, increasing the size of the ribs on the trailing wall increases the heat (mass) transfer on the leading wall.

2) For a fixed rib configuration on the trailing wall, increasing the size of the ribs on the leading wall does not significantly affect the heat (mass) transfer on the trailing wall.

3) With rotation at a relatively high speed, the heat (mass) transfer on the leading wall is quite low, regardless of the sizes of the ribs on the leading and trailing walls.

Acknowledgment

This study was sponsored by NASA Lewis Research Center, Cleveland, Ohio, Contract NAS3-27739.

References

[1]Park, C. W., Lau, S. C., and Kukreja, R. T., "Heat/Mass Transfer in a Rotating Two-Pass Square Channel with Transverse Ribs," *Journal of Thermophysics and Heat Transfer*, Vol. 12, No. 1, 1998, pp. 80–86.

[2]Goldstein, R. J., and Cho, H. H., "A Review of Mass Transfer Measurements Using Naphthalene Sublimation," *Experimental Thermal and Fluid Science*, Vol. 10, May 1995, pp. 416–434.

[3]Park, C. W., "Local Heat/Mass Transfer Distributions in Rotating Two-Pass Square Channels," Ph.D. Dissertation, Dept. of Mechanical Engineering, Texas A&M Univ., College Station, TX, Dec. 1996.

Thermal Contact Conductance of Elastomeric Gaskets

S. R. Mirmira,* E. Marotta,† and L. S. Fletcher‡
Texas A&M University,
College Station, Texas 77843-3123

Introduction

REMOVING heat from electronic components is a problem faced by engineers working on thermal management issues. To a very large extent, elastomeric gaskets have replaced mica pads and silicon greases as a means for enhancing the heat transfer across a material junction. With the miniaturization of electronic components and associated increase in power densities, the thermal contact resistance across junctions has assumed significant importance. There is limited information on the thermal contact conductance of these gasket materials. To provide some information on the thermal contact conductance of elastomeric gasket materials, which would prove extremely beneficial to thermal management engineers, the present investigation was conducted.

Presented as Paper 97-0139 at the AIAA 35th Aerospace Sciences Meeting, Reno, NV, Jan. 6–9, 1997; received Dec. 1, 1997; revision received March 9, 1998; accepted for publication March 10, 1998.

*Graduate Research Assistant, Conduction Heat Transfer Laboratory, Mechanical Engineering Department. Student Member AIAA.

†Currently Visiting Assistant Professor, Mechanical Engineering Department, Clemson University, Clemson, SC 29634-0921. Member AIAA.

‡Thomas A. Dietz Professor, Conduction Heat Transfer Laboratory, Mechanical Engineering Department. E-mail: LSF0290@acs.tamu.edu. Fellow AIAA.

Fletcher and Miller[1] conducted an experimental investigation on the thermal conductance of selected filled and unfilled elastomeric gasket materials. The thermal conductance values of all the elastomers tested were lower than the conductance of the bare aluminum junction. Furthermore, the investigation concluded that elastomers with metallic or oxide fillers yielded higher conductance values than unfilled elastomers.

Scialdone et al.[2] conducted an experimental investigation to measure the thermal contact conductance of polymeric materials that are suitable for electronic systems. Thermal contact conductance of Cho-Therm 1671, a silicone elastomer, and CV-2946, a conductive RTV silicone, were measured on a test configuration that attempted to simulate heat dissipation from a modular power system. A comparison of the thermal contact conductance between the two polymeric materials indicates that the RTV silicone compound (CV-2946) had higher values than the polymeric elastomer (Cho-Therm 1671).

Mirmira et al.[3] conducted an experimental study that measured the thermal contact conductance of adhesives (epoxies, silicone elastomer, and high-temperature air-set cements). Metalbond 1146 (BASF 1146) possessed the highest thermal contact conductance value of the different adhesives investigated. Norcast 3230HT possessed the highest thermal contact conductance value among the epoxies tested. The paper concluded that the mean interface temperature and apparent interface pressure do not significantly affect the thermal contact conductance value for a majority of adhesives tested. The only exception was the silver epoxy that registered an increase in conductance with an increase in pressure. Furthermore, at higher pressures, the thermal contact conductance value of the bare junction (aluminum 6101 and aluminum 356) was higher than that with the adhesive.

Experimental Program

To provide additional information on the thermal conductance of selected thermally conductive gasket materials, an experimental investigation was conducted. Several commercially available homogeneous gasket materials commonly used in aerospace applications were selected for this study. The gasket materials were cut in the form of precise 2.54 cm (1 in.) diameter discs of different thicknesses. Table 1 lists the material properties of the gasket materials as reported by the manufacturer.

The test facility used in this experimental investigation utilized a vertical column consisting of a frame with sliding plates for the support of two combination heat source/sink specimen holder assemblies, a load cell, and pneumatic bellows. A schematic diagram of the test facility and a description has been given by Mirmira et al.[3,4]

The vertical test column consisted of aluminum 6061-T6 upper and lower flux meters and a central aluminum 6061-T6 sample. The diameter of the flux meters and the sample were 2.54 cm (1 in.) and the lengths were 10.16 cm (4.0 in.) and 3.81 cm (1.5 in.), respectively. The thermally conductive gasket was placed at the interface between the aluminum 6061 central sample and the aluminum 6061 flux meter. The flux meters were instrumented with 30-gauge, Teflon/Teflon® sheath, special limit of error, K-type thermocouples.

Experimental Procedure

The aluminum 6061 flux meters and sample with the gasket positioned in between were inserted carefully into the test facility and aligned. The heat fluxes in the upper and lower flux meters as well as through the sample and gasket were determined by knowing the temperature gradients and thermal conductivities of the aluminum 6061 heat flux meters and sample. The difference in temperature at the gasket—flux meter interface was determined by extrapolating the temperature gradient in the heat flux meters to the gasket interface. The apparent interface pressure at each temperature was varied according to the hardness (Shore A) of the gasket being tested.